ORIGINAL ARTICLE

Cytoskeletal protein degradation in brain death donor kidneys associates with adverse posttransplant outcomes

Rebecca H. Vaughan[1,2] | Jean-Claude Kresse[3] | Louise K. Farmer[4] | Marie L. Thézénas[5] | Benedikt M. Kessler[5] | Jan H. N. Lindeman[6] | Edward J. Sharples[7] | Gavin I. Welsh[4] | Rikke Nørregaard[3] | Rutger J. Ploeg[1,2,6] | Maria Kaisar[1,2]

[1]Research and Development, NHS Blood and Transplant, Bristol & Oxford, UK

[2]Nuffield Department of Surgical Sciences, Oxford University Hospital Oxford, Biomedical Research Centre, University of Oxford, Oxford, UK

[3]Department of Clinical Medicine, Aarhus University, Aarhus, Denmark

[4]Bristol Renal, Bristol Medical School, University of Bristol, Bristol, UK

[5]Nuffield Department of Medicine, Target Discovery Institute, University of Oxford, Oxford, UK

[6]Department of Surgery, Leiden University Medical Centre, Leiden, The Netherlands

[7]Oxford University Hospital, Oxford, UK

Correspondence
Maria Kaisar, Nuffield Department of Surgical Sciences, University of Oxford, Oxford, UK.
Email: maria.kaisar@nds.ox.ac.uk

In brain death, cerebral injury contributes to systemic biological dysregulation, causing significant cellular stress in donor kidneys adversely impacting the quality of grafts. Here, we hypothesized that donation after brain death (DBD) kidneys undergo proteolytic processes that may deem grafts susceptible to posttransplant dysfunction. Using mass spectrometry and immunoblotting, we mapped degradation profiles of cytoskeletal proteins in deceased and living donor kidney biopsies. We found that key cytoskeletal proteins in DBD kidneys were proteolytically cleaved, generating peptide fragments, predominantly in grafts with suboptimal posttransplant function. Interestingly, α-actinin-4 and talin-1 proteolytic fragments were detected in brain death but not in circulatory death or living donor kidneys with similar donor characteristics. As talin-1 is a specific proteolytic target of calpain-1, we investigated a potential trigger of calpain activation and talin-1 degradation using human ex vivo precision-cut kidney slices and in vitro podocytes. Notably, we showed that activation of calpain-1 by transforming growth factor-β generated proteolytic fragments of talin-1 that matched the degradation fragments detected in DBD preimplantation kidneys, also causing dysregulation of the actin cytoskeleton in human podocytes; events that were reversed by calpain-1 inhibition. Our data provide initial evidence that brain death donor kidneys are more susceptible to cytoskeletal protein degradation. Correlation to posttransplant outcomes may be established by future studies.

KEYWORDS
basic (laboratory) research/science, cellular biology, donors and donation: donation after brain death (DBD), glomerular biology and disease, kidney (allograft) function/dysfunction, kidney failure/injury, kidney transplantation/nephrology, organ transplantation in general, proteomics, translational research/science, QUOD biobank

1 | INTRODUCTION

When compared to dialysis, transplantation profoundly increases life-expectancy, improves quality of life (QoL), and is cost-effective.[1–3]

Deceased kidney donation after brain death (DBD) is the main source of transplants, yet these grafts yield inferior short and long-term transplant outcomes when compared to living donation. This makes kidney allograft failure one of the most common morbidities to start dialysis in the United Kingdom and the United States.[4]

The process of brain death and subsequent donor management in intensive care units is associated with a complex homeostatic dysregulation in the donor[5,6] strongly suggesting that brain death negatively impacts organ quality.[7] In fact, brain death associates with a specific pattern of damage to renal substructures including the podocyte, which will compromise posttransplant graft function and graft survival.[8–14] As yet, the molecular processes underlying brain death-associated glomerular injury, with the potential for targeted interventions and pharmaceutical prevention, are unknown.[15]

Proteolytic damage of podocytes is a common effector pathway for glomerular diseases.[16–18] Recent studies in experimental models, suggest that the maintenance of renal filtration barrier largely relies on proteases as key regulators of podocyte integrity and kidney function.[19] Evidence that dysregulation of proteolytic pathways is a key driver for human disease signifying proteases as promising targets for tailored therapeutics.[20]

In this study, by utilizing the Protein Topography and Migration Analysis Platform (PROTOMAP),[21] we initially profiled the protein degradome (proteolytic modifications) of donor kidney biopsies that were selected on the basis of extreme paired transplant outcomes. Next, to visualize and better describe the detected proteolytic fragments, we analyzed a separate cohort of DBD, donation after circulatory death (DCD), and living donor kidney biopsies by immunoblotting. Finally, based on our previous research findings[22,23] and aiming to gather initial evidence of a potential trigger of cytoskeletal protein degradation, we investigated, using two complementary models of human ex vivo precision-cut kidney slices and in vitro human kidney podocytes, whether Transforming Growth Factor - β (TGF- β) calpain interaction may drive degradation of key structural proteins destabilizing the podocyte cytoskeleton.

2 | MATERIALS AND METHODS

2.1 | Clinical characteristics of donor cohorts

This study is based on the analysis of preimplantation kidney biopsies obtained from 65 deceased and living kidney donors. Deceased donor kidney biopsies were obtained from the Quality in Organ Donor (QUOD) biobank, a UK multicenter bioresource of deceased donor clinical samples procured during donor management and organ recovery.[24] Healthy living donor (LD) kidney biopsies were obtained from the Oxford Transplant Biobank (OTB).

Selection of donor kidneys was based on paired 12-month post-transplant outcomes. To minimize the impact of recipient factors on outcomes we only included kidneys for which the contralateral kidney was transplanted and had similar 12-month posttransplant outcome; either suboptimal (SO; eGFR ≤ 40 ml/min/1.73 m^2) or good outcome (GO; eGFR ≥ 50 ml/min/1.73 m^2). All clinical samples were linked to corresponding donor and recipient demographic and clinical metadata, provided by NHS Blood and Transplant (NHSBT) registry. Detailed clinical data are summarized in Table 1 and Table S1.

Biopsies were selected from one kidney per donor, either the left or right kidney, selected at random.

Deceased and living donor biopsies were collected according to the same stringent predefined collection protocols. Deceased and living donor kidney biopsies were collected ex situ immediately after flush-out and procurement of the kidney in the donor hospital on the back table. Biopsies were obtained from the upper pole of the donor kidney cortex, using a 23-mm needle biopsy gun. The obtained biopsies were then divided in two, with one half stored in RNAlater, then liquid nitrogen and the other half stored in formalin. All donor (deceased and living) kidney biopsies were procured, handled, and stored according to identical protocols, to minimize preanalytical variability and technical precautions were taken to eliminate ex vivo sample proteolysis.

For the initial degradomics profiling by PROTOMAP (detailed description in Supplementary Data M1.2), we analyzed two cohorts of pooled biopsy homogenates of DBD ($n = 10$) kidneys with contrasting transplant outcomes SO ($n = 5$) versus GO ($n = 5$) (Figure 1A,B). Degradomics data were confirmed by western blot (Supplementary Data M1.5) on an independent cohort of DBD ($n = 32$) donor kidneys. Biopsies from DCD donor kidneys ($n = 23$) with suboptimal outcomes (SO), good outcomes (GO), and from living donors (LD, $n = 10$) with good 12-month transplant outcomes were included as a reference cohort.

2.2 | PROTOMAP sample preparation

(Supplementary Data M1.1)[21,25]

2.3 | Protein Topography and Migration Analysis Platform and Data Analysis (PROTOMAP)

Kidney biopsies from the QUOD biobank were prepared and analyzed by PROTOMAP as previously described (Supplementary Data M1.2).[26–28]

2.4 | Preparation of precision cut kidney slices (PCKSs)

PCKSs were prepared from healthy renal cortical tissue obtained from patients following tumor nephrectomies, as described previously (Supplementary Data M1.3).[29]

TABLE 1 Donor and recipient characteristics

Donor characteristics	DBD			DCD			LD
	Suboptimal outcome (n = 16)	Good outcome (n = 16)	p value	Suboptimal outcome (n = 10)	Good outcome (n = 13)	p value	Good outcome (n = 10)
Age (y)	57 ± 10	48 ± 12	.02	51 ± 5	45 ± 12	.12	47 ± 11
Sex (%)							
Male	6 (38)	8 (50)	.72	8 (80)	7 (54)	.38	6 (55)
Race (%)							
White	16 (100)	16 (100)	1.0	10 (100)	12 (92)	1.0	10 (91)
Weight (kg)	84 ± 22	87 ± 19	.65	86 ± 10	72 ± 8	.001	
Height (cm)	166 ± 11	173 ± 11	.08	171 ± 7	173 ± 8	.54	
S-Cr terminal (μmol/L)	129 ± 116.3	75 ± 30	.28	88 ± 26	62 ± 21	.02	
S-Cr Outlier removed	81 ± 44	75 ± 30	.63				
Donor eGFR (ml/min/1.73 m^2)	81 ± 49	110 ± 47	.10	88 ± 30	119 ± 41	.06	
Donor cause of death (%)			.47			.09	N/A
Intracranial hemorrhage	10 (63)	6 (38)		3 (30)	10 (77)		
Intracranial event	3 (19)	1 (6)		1 (10)	1 (8)		
Hypoxia	2 (12)	4 (25)		3 (30)	2 (15)		
Cardiovascular		1 (6)					
Trauma - RTA		1 (6)		1 (10)			
Trauma - Suicide/Accident	1 (6)	2 (13)		1 (10)			
Other		1 (6)		1 (10)			
AKIN classification (%)			.89			.83	
No AKIN	13(82)	14(88)		8 (80)	12 (92)		N/A
1	1(6)	1 (6)		1 (10)			
2	1(6)	1 (6)					
3	1(6)	0					
Missing data				1(10)	1 (8)		
Warm ischemia time (min)				16 ± 3	36 ± 38	.19	
Duration : Admission/Cold perfusion (h)	107 ± 81	142 ± 120	.58	109 ± 57	144 ± 98	.34	N/A
Duration : Brain stem death/Retrieval (h)	16 ± 3	19 ± 7	.15				
Duration : Admission/Circulatory arrest (h)				109 ± 57	144 ± 99	.34	N/A
Duration : Circulatory arrest/Cold perfusion (min)				12 ± 5	19 ± 24	.87	N/A
CIT (h)	16 ± 6	14±4	.13	13 ± 7	13 ± 5	.82	N/A
KDPI (%)							
25th percentile	49	21		49	31		
75th percentile	86	60		81	76		
Early graft function (%)			.03			1.0	
Delayed graft function	15 (47)	6 (19)		2 (10)	5 (20)		
Immediate Function	17 (53)	22 (69)		12 (60)	17 (65)		
Unknown		4 (12)		6 (30)	4 (15)		
Post transplant kidney function (paired) eGFR ml/min/1.73 m^2			<.0001			<.0001	
3-months	31 ± 8	72 ± 15		31 ± 12	81 ± 21		
12-months	31 ± 9	82 ± 22		29 ± 9	77 ± 17		69 ± 10
Recipient serum creatinine mg/dL			<.0001			<.0001	
12-months	204 ± 55	90 ± 27		211 ± 66	101 ± 38		95 ± 20

2.5 | Cell culture

Conditionally immortalized human podocyte cell lines[30] were provided by the Bristol Renal Group at the University of Bristol, UK (Supplementary data M1.4)[31].

2.6 | Western blotting

(Supplementary Data M1.5)

2.7 | Calpain activity

(Supplementary Data M1.6)

2.8 | Cell imaging

(Supplementary Data M1.7)

2.9 | QPCR

(Supplementary Data M1.8)

2.10 | Sirius red staining and Masson's Trichrome staining

(Supplementary Data M1.9)

2.11 | Statistical analysis

The number of samples required to demonstrate meaningful changes between donor subgroups with extreme graft function either suboptimal or good outcomes has been calculated based on the effect size observed in previous work.[22] Taking into consideration that paired posttransplant outcomes reduces variability we calculated that an estimated minimum of $n = 8$ individual donor samples were needed to achieve $p < .05$, a statistical power 0.8% and a difference 0.2% on the expression of previously identified proteins between SO versus GO.

Statistics for this study were performed using Graph Pad Prism V7. Differences in continuous variables were analyzed using an ANOVA (more than two groups) or two-tailed unpaired Mann–Whitney test while discrete variables were analyzed using chi-squared tests. Minimum of three technical replicates were performed in each experimental analysis. Normalized intensities of immunoblotting data are shown as a mean ± SEM. Kidney Donor Profile Index was calculated using the online calculator https://optn.transplant.hrsa.gov/resources/allocation-calculators/kdpi-calculator

3 | RESULTS

3.1 | Clinical characteristics of deceased and living donors

Kidney biopsies were obtained from DBD, DCD, and living donors at the back table immediately after kidney procurement. To minimize the impact of cofounding factors related to post-procurement and recipient factors, donors were selected on the basis of paired 12-months posttransplant outcomes. Clinical metadata confirmed that the selected donor groups were representative of the donor population in the United Kingdom and shown limited clinical variability between donor subgroups (Table 1). The DBD SO group with median age (57 ± 10 years) was older than DCD SO (51 ± 5 years) but the age difference was not considered to be clinically significant. Intracranial event (trauma/hemorrhage) was the main cause of death for DBDs and DCDs. There were more DBDs with AKIN 2–3 than DCD, likely to reflect the uncertainty of clinicians in accepting DCD kidneys with AKIN > 1. Duration of donor admission to cold perfusion, WIT, and CIT were all comparable among all donor subgroups. KDPI profiles revealed clear differences in the 25th and 75th percentiles between SO and GO in both donor types, importantly there was no difference between DBDs and DCDs suggesting that donor factors in isolation could not explain the DBD-specific degradation observed for these specific proteins. In the associated metadata has been recorded that one of the DBD SO donors had a 5.4-fold increase of serum creatinine (from admission to terminal). This outlier value increased the mean value of DBD SO S-Cr to reach significance when compared to DBD GO. Exclusion of this outlier value resulted terminal S-Cr of DBD SO (81 ± 44) to be comparable to DCD SO (88 ± 26) (μmol/L). Recipients mean 3- and 12-month posttransplant eGFR were significantly different between SO versus GO (SO vs. GO; $p < .0001$).

3.2 | PROTOMAP shows degradation alterations in cytoskeletal proteins of donor kidneys with suboptimal transplant outcomes

Putative differences in the preimplantation kidney degradome of SO and GO DBD kidneys were mapped through the Protein Topography and Migration Analysis Platform (PROTOMAP)[25,32] (Figure 1B) (Supplementary Methods M1.1 and 1.2).

This analysis generated 15 700 peptographs corresponding to 6700 proteins. Stringent selection criteria (including the requirement for at least 20% protein sequence coverage for shortlisting proteins) reduced the data set to 2320 protein IDs and 1554 protein classes. Pathway analysis performed using (PANTHER 16.0) mapped 135 of these proteins as cytoskeletal and 65 of these linked to the integrin regulation pathway. Direct protein–protein interactions (STRING 6.0) showed enrichment of KEGG pathways of focal adhesion false discovery rate (FDR) 2.11 e-33, catabolic regulation FDR 1.06 e-09 and integrin-mediated signaling FDR 3.09e-9 (Figure S1).
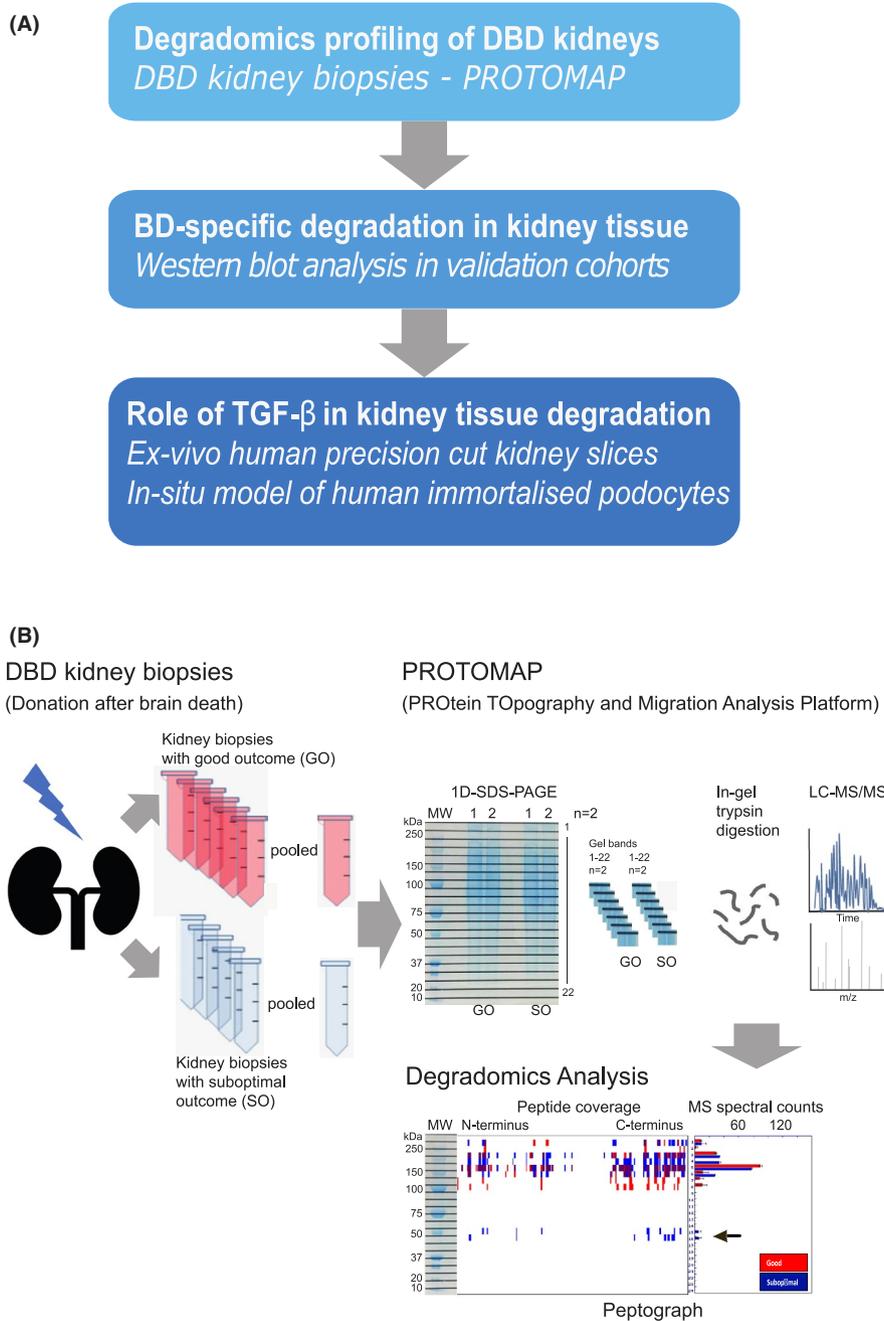
FIGURE 1 Experimental and technical workflows used in this study. (A) Study design. We first studied the degradation profiles of DBD kidneys that had contrasting 12-month posttransplant outcomes; either suboptimal (SO) or good allograft (GO) function. We applied the PROtein TOpography and Migration Analysis Platform (PROTOMAP) in kidney biopsies that were obtained from the QUOD biobank. The analysis shortlisted eight cytoskeletal proteins that were proteolytically cleaved in SO DBD kidneys. Western blotting on a validation cohort of deceased (DBD and DCD) and living donor (LD) kidney biopsies showed brain death–specific degradation patterns. To explain the degradation profiles, we tested the role of TGF-β in kidney tissue degradation by employing an ex vivo model of precision-cut human kidney slices and an in vitro model of human podocyte cells; (B) Description of the PROtein TOpography Migration Analysis Platform (PROTOMAP) workflow. DBD kidney biopsy protein homogenates were first separated by SDS-electrophoresis, divided into 224 horizontal sections and subsequently analyzed by LC–MS/MS. Bioinformatics analysis combined data from the gel electrophoresis and mass spectrometry spectra to generate peptographs that provided information on degradation profiles of the intact protein and the generated fragments. The resulting peptographs were screened to identify proteins with evidence of endogenous proteolysis and generation of fragment intermediates at a lower molecular weight than the full length. The selection of proteins for further analysis was based on the following factors: (i) increased spectral counts of fragments that had migrated at a lower molecular mass in SO (blue bars) versus GO (red bars), (ii) enrichment of the intact protein or protein fragments in the SO group and (iii) biological relevance, with an emphasis on cytoskeletal proteins

(A) Alpha Actinin

(B) Laminin subunit B2

(C) Talin

(D) Utrophin
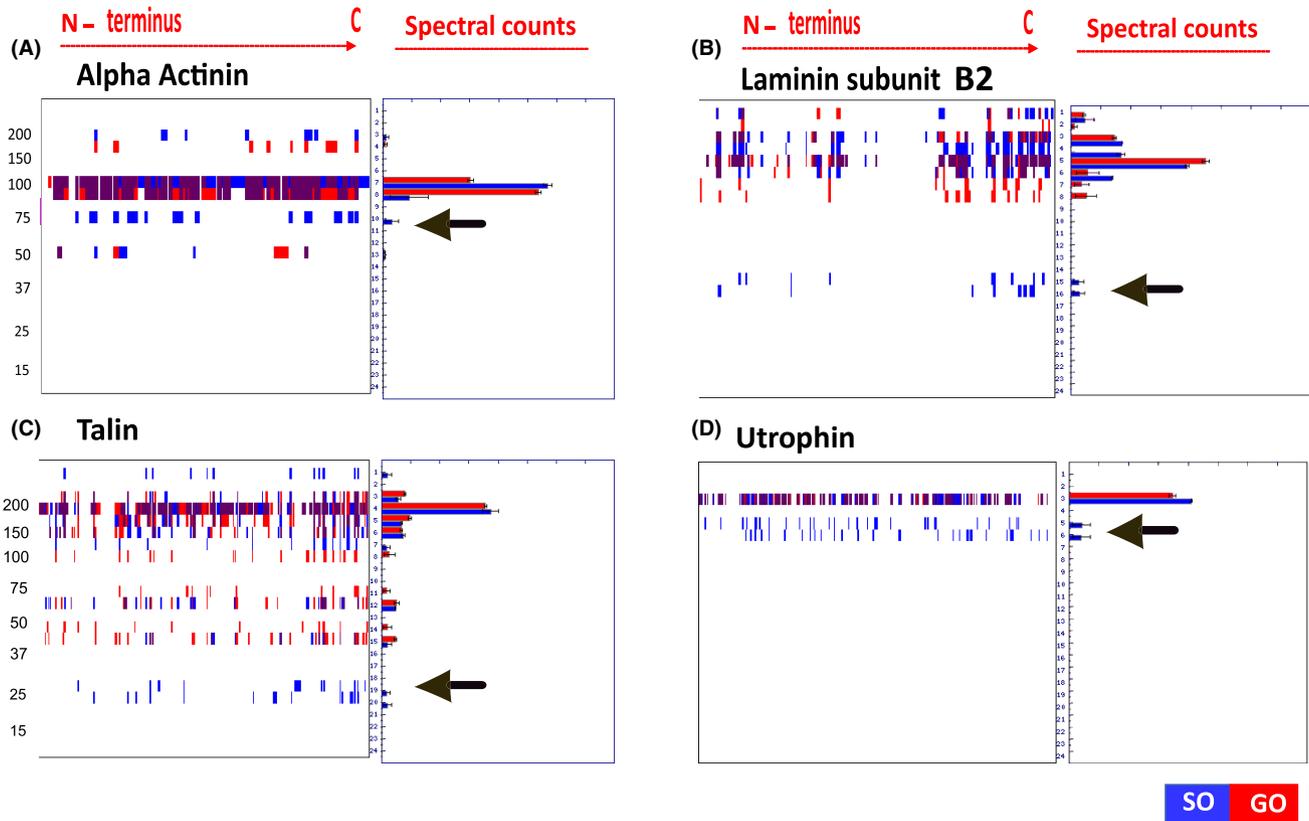
(E)
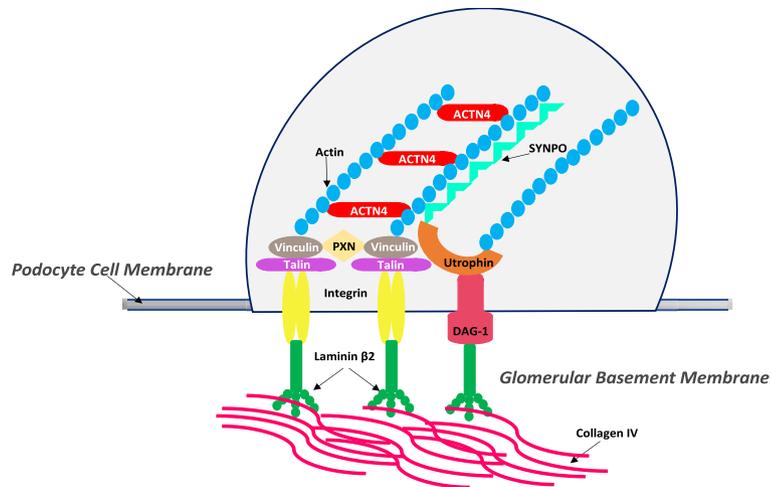
Podocyte proteins with distinct proteolytic profiles in DBD kidneys with SO 12-months posttransplant function	Full length protein (*)	Fragments generated from proteolytic cleavage of full length protein
A-actinin ^	105 KDa	90-70 & 40-30 KDa
Talin ^	270 KDa	125, 25 KDa
Utrophin	> 390 KDa	190, 150 KDa
Laminin subunit β2	200 KDa	45 KDa

To identify evidence of increased proteolysis in donor kidneys, we scanned the peptographs of the cytoskeletal proteins to detect the generation of lower molecular mass fragments of intact proteins in SO kidneys (blue bars) not observed in GO kidneys (red bars) (Figure 2). Eight proteins mapped to podocyte cytoskeleton; α-actinin-1, −4, talin-1, −2, utrophin, laminin β2, synaptopodin, integrin α-1, showed specific and contrasting degradation profiles for SO when compared to GO grafts (Figure 2, Figures S1 and S2). To confirm protein degradation detected in PROTOMAP data and further investigate whether there were donor type specific differences in the degradome, we performed a targeted analysis of α-actinin-4 and talin-1 by western blot on deceased and living donor kidney biopsies. The cohort of samples selected for blotting was independent of the samples pooled to PROTOMAP analysis.

FIGURE 2   Mapping the generation of protein fragments using PROTOMAP analysis of kidney biopsies. Arrows show the protein fragments detected in lower molecular weight generated from the full-length protein. Blue depicts suboptimal outcome (SO) kidneys and red depicts good outcome (GO) kidneys. Peptographs depict proteins shortlisted from the PROTOMAP analysis of DBD kidneys with GO (red bars) pooled $n = 5$; compared to biopsies obtained from DBD kidneys with SO (blue bars) pooled $n = 5$. Degradation profiles (noted with the arrow) from N terminus to C terminus of α-actinin (A), laminin β2 (B), talin (C), utrophin (D). (E) Podocyte schematic showing intracellular actin filaments linked to α-actinin-4 (ACTN4), synaptopodin (SYNPO), utrophin, talin, and through Integrins with intertwined laminin β2 podocyte connected to the podocyte basement membrane (peptographs of Integrin and synaptopodin listed in SF2). The table shows the full length and fragments identified from PROTOMAP analysis. As α-actinin-1/-4 isoforms and talin-1/-2 isoforms share 85% and 76% homology we included both isoforms of each protein in the analysis. *Indicates the full-length protein. ^Indicates that α-actinin and talin were validated by western blot on an independent cohort of biopsies and the association of the degradomics profiles to protein isoforms of α-actinin-4 and talin-1 were confirmed. (The separate protein isoform peptographs of α-actinin and talin in addition to the rest of the peptographs are displayed in Figure S2)
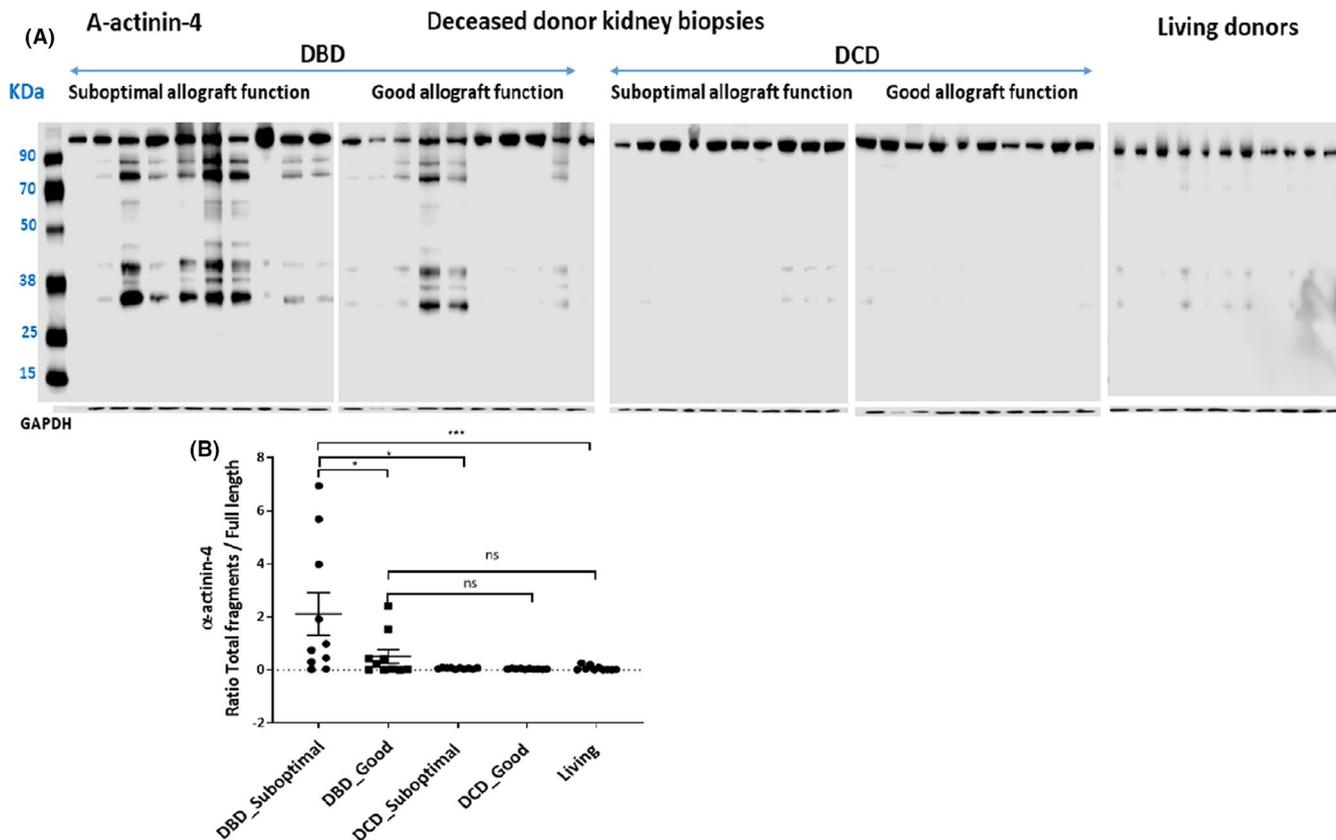

FIGURE 3   α-Actinin-4 proteolytic profile is specific to DBD kidneys and associates to posttransplant outcome. (A) Western blot analysis of donor kidney biopsies from $n = 10$ DBD with suboptimal outcome (SO: 12-month eGFR (±SD) 31 ± 9 ml/min/1.73 m^2), $n = 10$ DBD with good outcome (GO: 12-month mean eGFR (±SD) 82 ± 22 ml/min/1.73 m^2), $n = 10$ DCD with SO (12-month mean eGFR (±SD) 29 ± 9 ml/min/1.73 m^2 $n = 10$ DCD with GO 12-month mean eGFR (±SD) 77 ± 17 ml/min/1.73 m^2, and biopsies from $n = 10$ LD (12-month eGFR (±SD) 69 ± 10 ml/min/1.73 m^2) shows that the degradation of α-actinin-4 is specific to DBD kidneys while DCD and LD kidneys show no evidence of degradation. α-Actinin-4 shows a distinct profile of fragments generated between 90 and 70 kDa and between 40 and 30 kDa. (B) The ratio of total fragment intensities (normalized to GAPDH) to the full-length protein (105 KDa) shows that the proteolytic processing of the DBD kidneys with SO is significantly different to DBD GO (means ± SEM, *$p < .05$), the DBD SO is significantly different to DCD SO and LD (means ± SEM, *$p < .05$; ***$p < .001$) while there was no difference in the degradation pattern between DCD and LD [Color figure can be viewed at wileyonlinelibrary.com]

3.3 | Immunoblotting suggest a link of cytoskeletal protein degradation to brain death

Western blots of α-actinin-4 and talin-1 of tissue homogenates from SO and GO DBD kidneys ($n = 32$) confirmed the degradome

findings (Figures 3 and 4) (Supplementary Methods M1.5). To explore whether the degradation signatures were altered in the different donor types, we also profiled kidney biopsies from SO and GO DCDs ($n = 23$), and from LDs ($n = 10$).

First, we examined the peptidomic profile of α-actinin-4 due to its pivotal role in maintaining healthy podocyte function.[18,33]
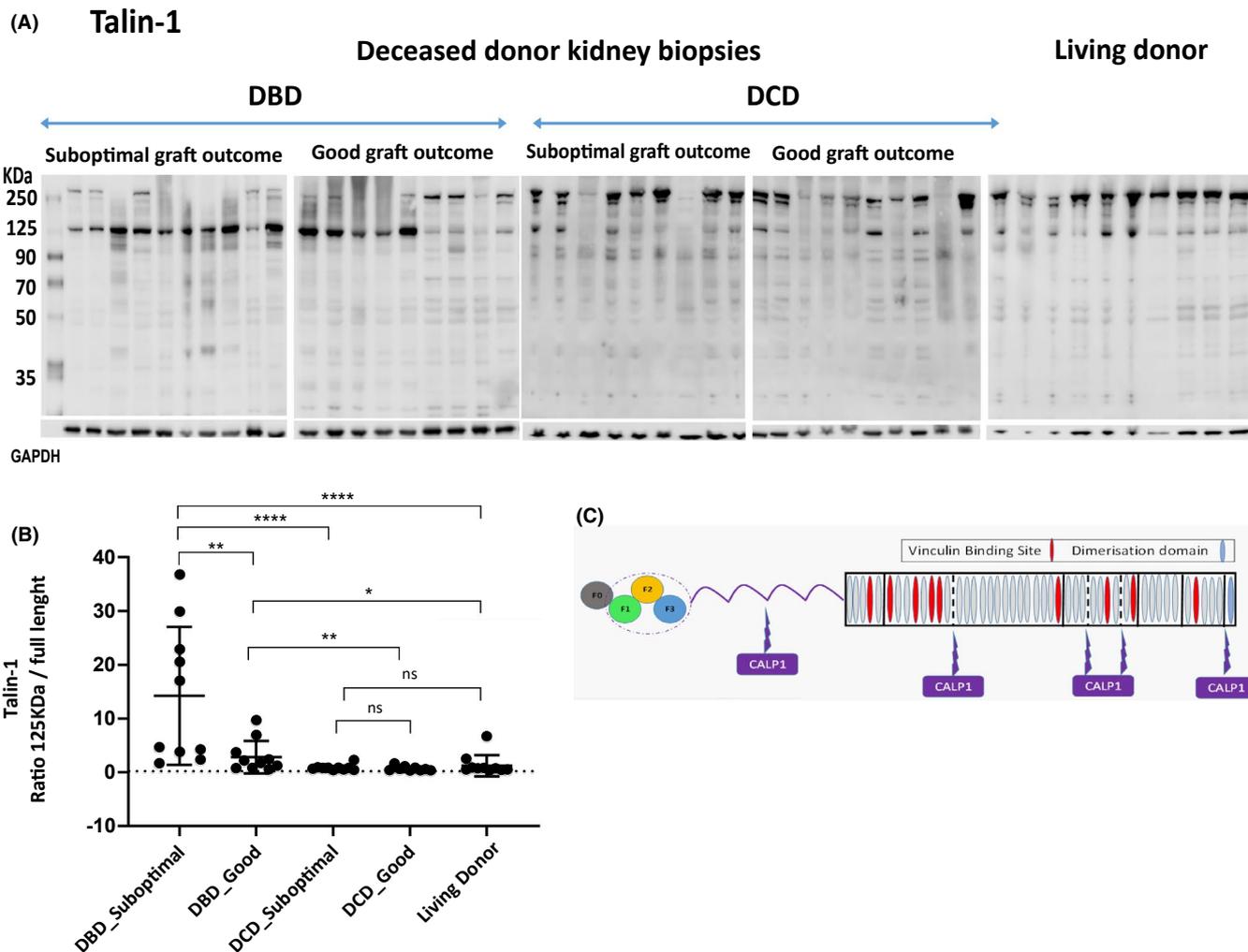
FIGURE 4 Talin-1 proteolytic profile is specific to DBD kidneys and associates to posttransplant outcome. (A) Western blot of donor kidney biopsies from $n = 10$ DBD with suboptimal outcome (SO: 12-month eGFR [±SD] 31 ± 9 ml/min/1.73 m^2), $n = 10$ DBD with good outcome (GO: 12-month mean eGFR [±SD] 82 ± 22 ml/min/1.73 m^2), $n = 10$ DCD with SO (12-month mean eGFR [±SD] 29 ± 9 ml/min/1.73 m^2), $n = 10$ DCD with GO (12-month mean eGFR [±SD] 77 ± 17 ml/min/1.73 m^2), and biopsies from $n = 10$ LD (12-month eGFR [±SD] 69 ± 10 ml/min/1.73 m^2) shows that the degradation of talin is specific to DBD kidneys. A fragment at 125 kDa is clearly increased with the degradation of the full-length talin protein at 270 kDa in the DBD kidneys. An additional fragment at 100 kDa was also observed in the DBD SO kidney. The 125-kDa fragment was detected in the DCD and LD kidneys also however in both donor groups the full-length protein was clearly distinct. (B) The ratio of total fragment intensities (normalized to GAPDH) to the full-length protein (270 kDa) shows that the proteolytic processing of the DBD kidneys with SO is significantly different to DBD GO (means ± SEM, **$p < .01$), the DBD SO is significantly different to DCD SO and LD (means ± SEM, ****$p < .0001$) while there was no difference in the degradation rates between DCD and LD. (C) Talin consists of an N-terminal head and a flexible rod. The head and rod are joined by a linker region that is cleaved by calpain [Color figure can be viewed at wileyonlinelibrary.com]

The profile of α-actinin-4 showed clearly that protein degradation had occurred only in DBD kidneys but not in DCD or LD kidneys (Figure 3A). The detected fragments generated from the full-length 105-kDa protein were significantly enhanced in SO, compared to GO DBD kidneys ($p < .05$), to DCD ($p < .05$) and LDs ($p < .001$) (Figure 3B).

Next, we surveyed the degradome profile of talin-1 due to its key structural role in linking integrins to the actin cytoskeleton.[34,35] The peptidomic profile of talin-1 demonstrated that in DBDs the full-length 270-kDa talin-1 protein was proteolytically processed in most of the DBD samples (Figure 4A) with the generation of ~100- to 125-kDa fragments. The intensity of the generated talin-1 fragments was calculated as the ratio of fragments to full-length protein, normalized against GAPDH loading controls. The generated fragments were significantly different in SO DBDs compared to GO DBDs, DCDs, and LD (Figure 4B).

Talin-1 is a specific target protein for the non-lysosomal cysteine protease calpain[36] with at least four calpain cleavage sites (Figure 4C). To further investigate proteolytic cleavage of talin-1, we investigated calpain activation in DBD kidneys with SO and GO outcomes.
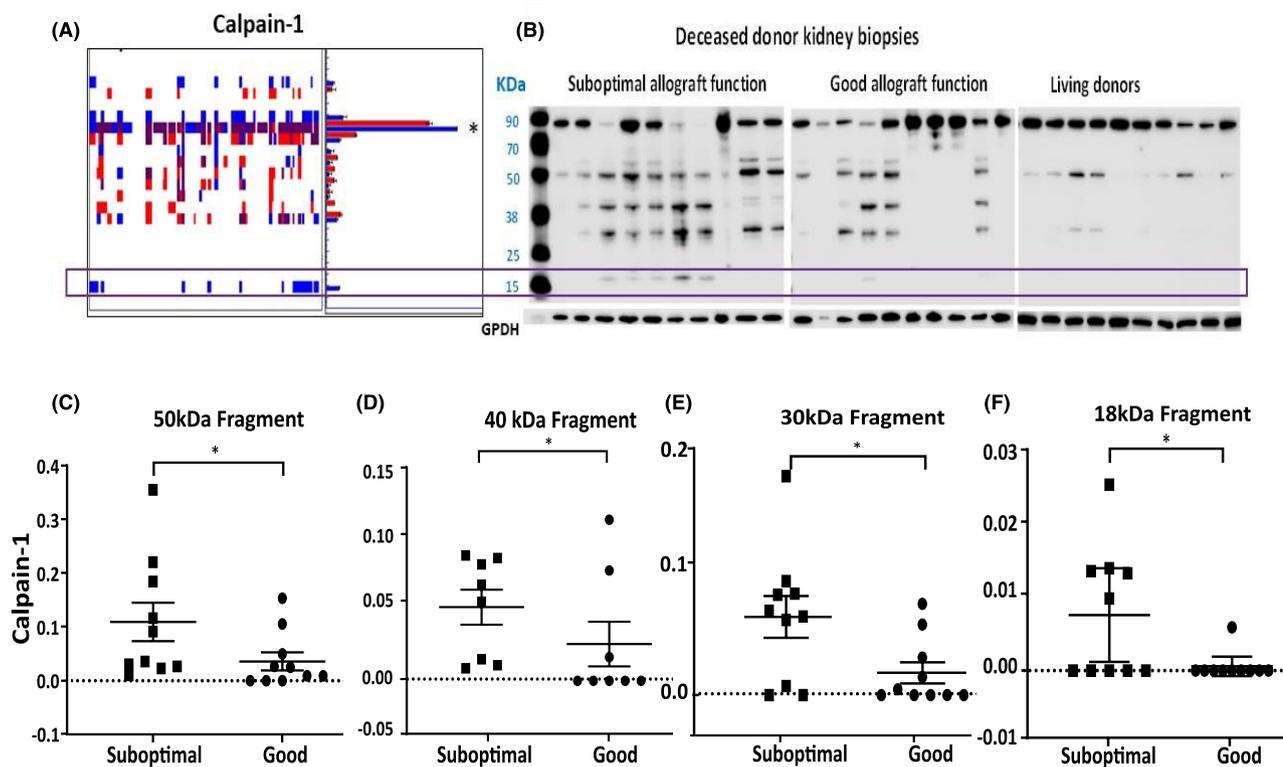
FIGURE 5 Calpain-1 peptidomic profile reveals enhanced enzymatic activation in suboptimal outcome DBD kidneys. (A) PROTOMAP analysis showed the generation of a number of fragments in DBD suboptimal outcome (SO) donor groups and the generation of a unique fragment at around 18 KDa in SO donor kidney biopsies. (B) Western blot analysis of donor kidney biopsies from $n = 10$ DBD with SO (12-month eGFR [$\pm$SD] 31 $\pm$ 9 ml/min/1.73 m^2), $n = 10$ DBD with good outcome (GO; 12-month mean eGFR [$\pm$SD] 82 $\pm$ 22 ml/min/1.73 m^2) showed distinct peptidomic profiles that included the generation of protein fragments increased at around ~50 kDa (C), ~40 kDa (D), ~30 kDa (E), and of a unique 18-kDa fragment (F) in SO when compared to GO DBD kidneys (means $\pm$ SEM, *$p < .05$; t-test). Band intensities were normalized against GAPDH
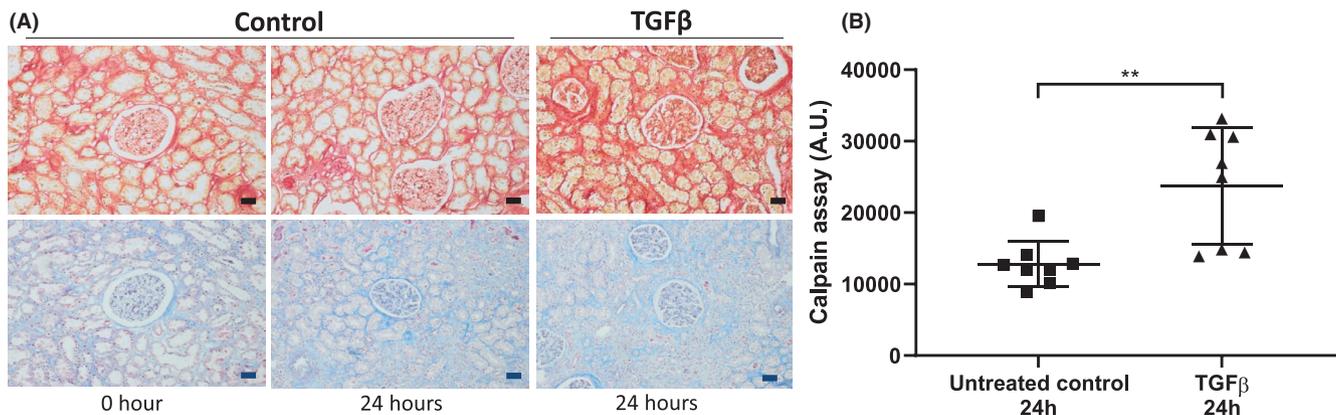

FIGURE 6 TGF-β treatment of human precision-cut kidney slice (PCKSs) increases calpain activity and caused pro-fibrotic morphological changes. (A) PCKSs stimulation with TGF-β (10 ng/ml) up to 24 h caused the kidney slices to develop pro-fibrotic morphological changes detected by Sirius red (top) and Masson's Trichrome staining (bottom). 20 × magnification and 20 μm scale bar. (B) Calpain-1 activity significantly (means $\pm$ SEM, **$p < .01$; paired t-test) increased in PCKSs treated with TGF-β up to 24 h

3.4 | Peptidomic alterations of calpain-1 indicate enzymatic activation

Our PROTOMAP data revealed that calpain-1 had a distinct fragmentation profile in SO kidneys compared to GO DBD (Figure 5A). This was confirmed by western blot analysis on a separate sample

cohort (Figure 5B) that showed that observed fragment intermediates at ~50, 40, and 30 kDa were significantly increased in SO when compared to GO DBDs ($p < .05$) (Figure 5C–E). A distinct fragment ~18 kDa was only seen in SO DBD kidneys (Figure 5F). The calpain-1 fragments (50, 40, 30, and 18 kDa) seen enriched in SO DBDs have been previously reported to be associated with calpain-1 enzymatic
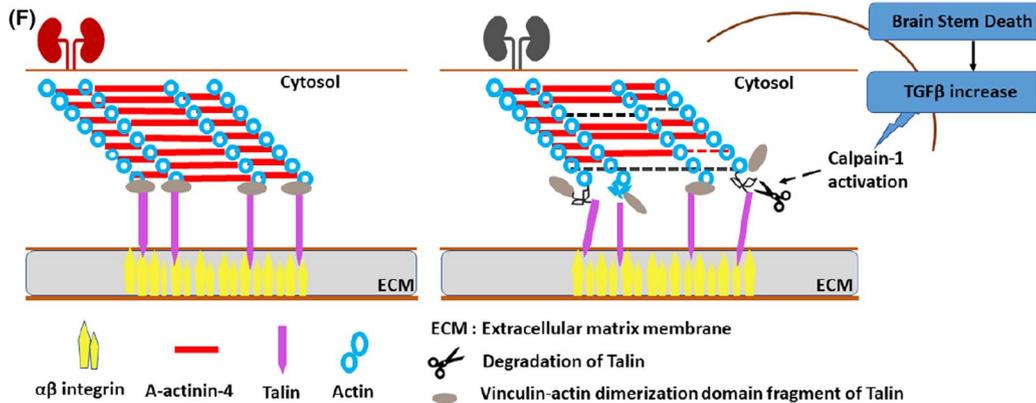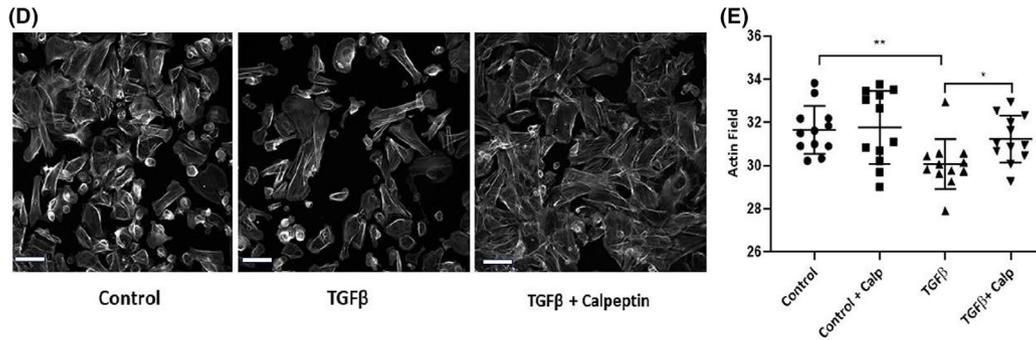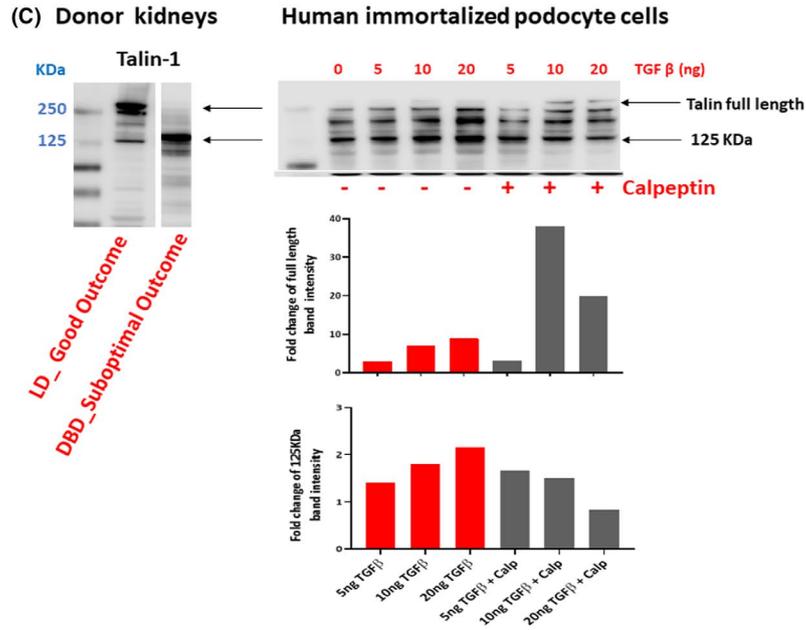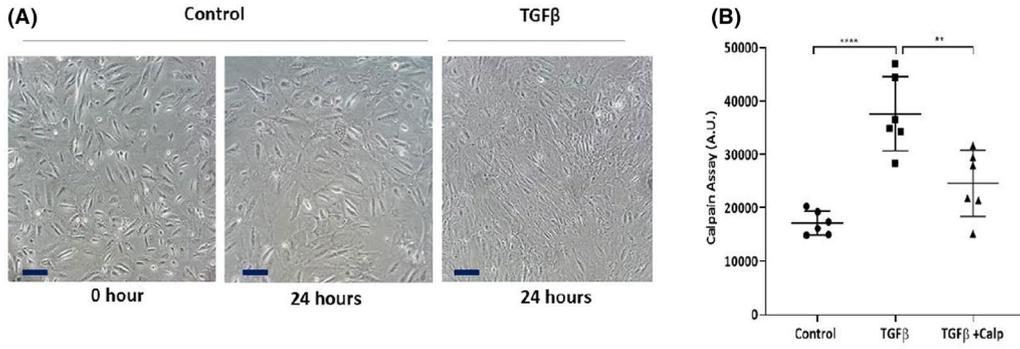
(A)

Control

0 hour   24 hours

TGFβ

24 hours

(B)

(C) Donor kidneys   Human immortalized podocyte cells

Talin-1

LD _ Good Outcome

DBD_Suboptimal Outcome

(D)

Control   TGFβ   TGFβ + Calpeptin

(E)

(F)

αβ integrin   A-actinin-4   Talin   Actin

ECM : Extracellular matrix membrane

Degradation of Talin

Vinculin-actin dimerization domain fragment of Talin

FIGURE 7 TGF-β treatment of human immortalized podocyte cells triggers calpain activation, actin cytoskeleton dysregulation and cytoskeletal talin degradation. (A) Representative contrast microscopy images showing changes to podocyte cells morphology when treated by TGF-β (10 ng/ml) for up to 24 h; 20× magnification, scale bar is 100 μm. (B) Calpain activity of podocyte cells was significantly increased following stimulation with TGF-β (10 ng/ml) up to 24 h when compared to control (****$p < .0001$; t-test). Treatment of cells with calpeptin (1 μM) prior to and during TGF-β stimulation significantly reduced calpain activation (**$p < .01$; t-test). (C) The degradation pattern of talin-1 of suboptimal DBD kidneys compared to LD kidney with good outcome showed the generation of ~125-kDa fragment (cropped western blot presenting donor kidneys probed with anti-talin-1 was derived from data presented in Figure 4A). In vitro human kidney podocyte cells stimulated with TGF-β (0-20 ng/ml, up to 24 h) showed a dose responsive loss of the talin full-length protein. Talin-1 proteolytic fragments were detected as ~190- and ~125-kDa bands with a further lower intensity band at ~100 kDa. The generation of these fragments was reduced when podocytes were treated with calpain inhibitor calpeptin (1 μM) prior to and during TGF-β treatment. The two histograms show the alterations (fold changes) in the band intensities of the talin-1 main band and the 125-kDa fragment following treatment of podocytes with TGF-β in the absence (red bars) and presence of calpain-1 inhibitor calpeptin (gray bars). (D) Phalloidin staining of actin stress fibers in cultured conditionally immortalized podocytes in response to TGF-β (10 ng/ml) and calpeptin (1 μM) treatments (three technical replicates). (E) TGF-β treatment (10 ng/ml) decreased the length of actin fibers (**$p < .01$; t-test) indicating dysregulation of the actin cytoskeleton. This loss of stress fiber area was recovered by treating cells with 1 μM calpeptin alongside the TGF-β treatment (*$p < .05$; t-test). 10× magnification and 20 μm scale bar. (F) Schematic representation of the podocyte cytoskeletal matrix of healthy and after brain death kidney; brain stem death increases TGF-β triggering the activation of calpain-1 and subsequent degradation of cytoskeletal talin-1 affecting the integrity of actin cytoskeleton in the kidneys with suboptimal posttransplant function

activation and subsequent autolytic processing.[37,38] As we were unable to perform calpain activity assays in tissue homogenates,[39] we used an ex vivo model of precision- cut human kidney slices and an in vitro model of immortalized human kidney podocyte cells to first validate our findings and then to explore a potential causal pathway to explain the degradomics patterns in DBD kidney biopsies.

3.5 | TGF-β treatment of precision-cut human kidney slices (PCKSs) increases calpain protease activity

We have previously shown increased levels of TGF-β in preimplantation DBD kidney biopsies with SO posttransplant outcomes[22] and as TGF-β plays a key role in preimplantation podocyte injury,[40] we hypothesized that TGF-β might trigger calpain activation. To investigate this, we used a novel ex vivo model of precision-cut human kidney slices (PCKS) that reflects closely the human kidney physiology (Figure 6A) (Supplementary Methods M1.3 and 1.8). Treatment of PCKSs with TGF-β significantly increased calpain activity ($p < .01$) compared to the untreated control in the first 24 h of treatment (Figure 6B) (Supplementary Methods M1.6). To further confirm the impact of TGF-β on PCKSs, we identified increased levels of collagen 1A1 mRNA suggesting that PCKSs had undergone interstitial collagen deposition and increased tubulointerstitial fibrosis; further confirmed by staining with Sirius Red and Masson's Trichrome-stained sections (Supplementary Data M1.9 and Figure S3).

3.6 | TGF-β treatment of human kidney podocytes-generated proteolytic fragments of talin-1 that matched DBD preimplantation kidney degradation profiles

To determine whether TGF-β-linked calpain-1 activation has a downstream impact on the integrity of the podocyte cytoskeleton, we employed an in vitro model of conditionally immortalized human kidney podocyte cells to investigate the impact of TGF-β stimulation for up to 24 h (Supplementary Methods M1.4). Induced cytoskeletal changes manifested as pro-fibrotic morphological alterations including cell elongation and thickening of the peritubular area (Figure 7A). Importantly, stimulation of podocytes with TGF-β caused significant calpain activation ($p < .0001$) (Figure 7B). Treatment of podocyte cells with calpain-specific inhibitor, calpeptin (1 μM), prior to and during stimulation with TGF-β, prevented TGF-β-induced calpain activation (Figure 7B).

Given the key role of talin-1 in sustaining the podocyte integrity and since we have shown that talin-1 was markedly degraded in DBD SO kidneys, we examined whether the interaction of TGF-β and calpain-1 led to degradation of talin-1 in this in vitro model.

Analysis by western blot of TGF-β-treated podocyte homogenates revealed that talin-1 was proteolytically processed with the generation of distinct fragments at ~190, ~125, and ~100 kDa (Figure 7C). Notably, the ~125-kDa fragment we had previously shown to be distinct in the DBD SO (Figure 4A) kidney biopsies with corresponding degradation of the full-length protein (Figure 7C), was also generated in podocytes in a TGF-β concentration-dependent manner. Inhibition with Calpeptin prior and during TGF-β stimulation, reduced the proteolytic processing, limited the generation of the 125-kDa fragment and reduced cleavage of full-length talin-1 (Figure 7C). This result strongly suggested that talin-1 degradation in this model was mediated by calpain, activated in turn by the treatment of podocyte cells with TGF-β (Figure 7C).

As podocyte cytoskeletal integrity is a key determinant of kidney disease; we examined whether TGF-β treatment impacted actin remodeling. Following TGF-β stimulation of podocyte cells, there was significant reduction of the actin stress fibers compared to the untreated cells ($p < .01$) and TGF-β+calpeptin-treated cells ($p < .05$) as measured by rhodamine phalloidin staining (Figure 7D,E) (Supplementary Methods M1.7). Taking together, these data show that TGF-β triggered calpain activation that negatively impacted the integrity of the podocyte actin cytoskeleton. The observed impact was inhibited by calpain inhibition, preserving the podocyte cytoskeleton.

4 | DISCUSSION

Our data, obtained from a unique cohort of preimplantation biopsies from DBD, DCD, and LD kidneys, provide initial evidence that activation of proteolytic processes predominantly occur in brain death causing alterations in podocyte cytoskeleton. Replicating the observed DBD kidney key degradation profiles of talin-1 in human kidney immortalized podocyte cells revealed a role of the calpain-1-TGF-β axis in proteolytic activation and cytoskeletal dysregulation that may deem grafts susceptible to subsequent injury–a causal link that further studies should aim to establish.

To investigate the donor kidney degradome we analyzed deceased and living donor kidney biopsies obtained with identical procurement protocols to minimize preanalytical confounding factors. This stringent experimental selection, based on paired transplant outcomes, also increased our confidence in obtaining meaningful data that predominantly relates to donor minimizing the impact or bias from surgical or posttransplant factors.

We, and more recently others, have shown that the application of the PROTOMAP technique to complex clinical samples provides a comprehensive profiling of both N- and C-terminal proteoforms with sufficient sequence coverage to determine epitope coverage by commercial antibodies, thereby allowing validation by immunoblotting.[25,41,42] Initial, unbiased PROTOMAP degradation profiling and pathway analysis mapped α-actinin, synaptopodin, talin, laminin β2, integrin α1, and utrophin as a cluster of cytoskeletal proteins associated with focal adhesion in podocytes had undergone enhanced proteolytic processing in DBD kidneys with SO posttransplant function. Evidence that proteolytic cleavage of key podocyte proteins is a destabilizing process that damages the integrity of podocytes and the glomerular filtration barrier has been previously shown in experimental models but with limited evidence on human kidneys to date.[20,43] Therefore, to further investigate protein degradation of the podocyte cytoskeleton and to better visualize donor-specific degradation patterns, we examined the degradome profiles for certain proteins on a separate cohort of donor kidney biopsies obtained from DBDs, DCDs, and LDs, by western Blotting. Blotting confirmed our PROTOMAP data showing that DBD-specific α-actinin-4 and talin-1 had undergone proteolytic processing and peptide fragments were enriched in suboptimal outcome grafts.

Although these two actin-binding proteins had been previously identified, mainly in vitro and preclinical settings, as susceptible to proteolysis,[18,34,44–47] here we show, that for these proteins, proteolytic modifications happen predominantly in DBD kidneys. Talin-1 and α-actinin-4 have a pivotal role in sustaining the normal kidney physiology[48] through either integrin activation and also in linking integrins to actin cytoskeleton. Consequently, talin-1 cleavage decouples integrins to actin cytoskeleton resulting in podocyte injury and kidney pathology, as previously described.[34,49–57] In our study, proteolytic cleavage of the full-length talin-1 protein with the parallel generation of the distinct ~125-kDa fragment, was clearly observed not only in kidney biopsies, but it was also confirmed in the in vitro human cell

model treated with TGF-β. We observed that in DCDs and LDs the ~125-kDa talin-1 protein fragment co-existed with the talin-1 full-length protein that appeared intact in most samples of these donor cohorts. This suggests that the generation of the ~125-kDa fragment may also results from normal protein turnover as part of the physiological maintenance of cellular homeostasis. In contrast, for the majority DBD kidneys, the ratio of the 125-kDa fragment compared to talin-1 full-length protein clearly shown that talin was proteolytically processed predominantly in SO DBD kidneys when compared to GO DBDs, DCDs, and LDs. As our study was not statistically powered to establish a causal link between proteolytic degradation and subsequent development of graft dysfunction a larger study is needed to confirm the observed associations of cytoskeletal degradation to suboptimal transplant outcomes.

As talin-1 is a specific calpain-1 target[36,58] and our PROTOMAP and western blot data indicate increased enzymatic activation of calpain-1 in DBD SO kidneys, our investigation focused on studying this interaction further using two complementary models. To investigate a possible trigger for calpain activation in DBD kidneys we built on our previous findings showing that TGF-β signaling is predominant in DBD kidneys when compared to DCDs and enhanced in SO DBDs.[22,23]

We demonstrated that TGF-β stimulation of both ex vivo precision-cut kidney slices and in vitro podocytes-mediated calpain-1 activation. In vitro calpain-mediated talin-1 degradation produced a ~125-kDa proteoform. This fragment was of the same size as the fragment detected in the DBD kidney biopsies indicating that full-length talin-1 had been cleaved by calpain-1 at the same cleavage site to produce the same size fragment. The role of calpain in this cascade was confirmed by the protective effect of calpeptin, a calpain-specific inhibitor.

Calpain proteases are tightly regulated and only activated directly by increased levels of intracellular levels of Ca^{+2}, micromolar levels favors calpain-1 activation.[37] Their physiological roles include cytoskeletal remodeling, cell cycle regulation, and apoptosis in addition to proteolysis of specific targets.[59] Calpain-1 is known to proteolytically target utrophin, α-actinin-4, and dystroglycan.[37] Calpain-mediated degradation of Utrophin[60] in muscle cells is reported to generate a ~190-kDa intermediate that we also detected in our PROTOMAP data.

Previously has been shown that TGF-β-mediated calpain activation has a role in endothelial mesenchymal transition to myofibroblasts and onset of fibrosis[61,62]; here our data indicate that multifaceted TGF-β has also a role in activating calpain-associated proteolytic pathways that alter the podocyte cytoskeletal integrity.

In our experiments, calpeptin markedly reduced TGF-β-driven degradation and prevented actin cytoskeletal dysregulation. As calpeptin has previously shown that ameliorates glomerular injury, in rodent and in vitro models of experimental focal segmental glomerulosclerosis,[31,63] our data may provide an insight of this protective mechanism.

As our data relate to deceased donor kidneys, it is important to consider our findings in the context of dysregulation following brain death. Severe cerebral injury, cerebral ischemia, and brain stem death cause the release of endogenous cytokines and catecholamines that

trigger a "sympathetic or catecholamine storm".[12,64,65] Circulating inflammatory mediators cause the activation of proteolytic pathways as previously described by others. These biological stressors trigger various cell stimuli such as membrane depolarization causing increased intracellular Ca^{2+} influx.[66] Once calpain is activated from changes in intracellular Ca^{2+}, it triggers proteolytic pathways that cleave key proteins, modifying the integrity of the podocyte cytoskeletal matrix in donor kidneys, as our data demonstrated. Determining whether cytoskeletal matrix protein degradation is ongoing posttransplant, thereby contributing to progressive development of allograft dysfunction, will open new therapeutic opportunities.

Emerging interest in the therapeutic application of calpain inhibition to treat diseases such as muscular dystrophy, neurological injury, and ischemia/reperfusion injury,[67] suggest a potential therapeutic strategy to modulate or inhibit calpain activation preventing podocyte damage in donor grafts early after brain death.

Although we detected well-defined differences between DBD and DCD kidneys in the level of cytoskeletal protein degradation, it will be inappropriate to make any broad suggestions to link donor type with overall organ quality. Multicollinearity of molecular and clinical factors in determining biological processes and clinical outcomes need to be further investigated in larger donor cohorts. It is highly probable that the complex biological changes during brain death and donor management disproportionally impacting donors with undiagnosed co-morbidities, deem these grafts susceptible to proteolysis and kidney injury.

As our observations derived from the analysis of clinical samples, inevitably we were faced with limitations related to biological heterogeneity, that may explain that in some donors talin detection was low. This might also be explained by heterogeneity in the number of glomeruli in the analyzed preimplantation biopsies.

In conclusion, our data indicate that brain death donor kidneys are more susceptible to cytoskeletal protein degradation that may predisposes grafts to further injury posttransplant. Further investigation should aim to unravel the role of TGF-β and calpain-1 interactions in protease activity in kidney disease. Defining how donor and recipient factors impacting proteolytic processes is essential as podocyte cytoskeletal degradation emerging as a novel mechanism of kidney injury.

ACKNOWLEDGMENTS

DISCLOSURE

The authors of this manuscript have no conflicts of interest to disclose as described by the *American Journal of Transplantation*.

AUTHOR CONTRIBUTION

MK conceptualized the study. RHV, GIW, RN, BMK, RJP, and MK designed the research. RHV, JCK, LKF, JIL, and MLT performed the experimental work. GIV, RN, ES, BMK, RJP, and MEK analyzed and interpreted the data. RHV, BMK, RJP, and MK wrote the manuscript. All authors revised the final manuscript.

DATA AVAILABILITY STATEMENT

The mass spectrometry proteomics data have been deposited to the ProteomeXchange Consortium via the PRIDE partner repository with the dataset identifier PXD022074 and 10.6019/PXD022074.

ORCID

Benedikt M. Kessler https://orcid.org/0000-0002-8160-2446
Gavin I. Welsh https://orcid.org/0000-0002-2148-6658
Rikke Nørregaard https://orcid.org/0000-0002-0580-373X
Rutger J. Ploeg https://orcid.org/0000-0001-7801-665X
Maria Kaisar https://orcid.org/0000-0002-0712-9937

REFERENCES

1. Oniscu GC, Ravanan R, Wu D, et al. Access to Transplantation and Transplant Outcome Measures (ATTOM): study protocol of a UK wide, in-depth, prospective cohort analysis. *BMJ Open*. 2016;6(2):e010377. doi:10.1136/bmjopen-2015-010377
2. Oniscu GC, Brown H, Forsythe JLR. Impact of cadaveric renal transplantation on survival in patients listed for transplantation. *J Am Soc Nephrol*. 2005;16(6):1859–1865. doi:10.1681/ASN.2004121092
3. Axelrod DA, Schnitzler MA, Xiao H, et al. An economic assessment of contemporary kidney transplant practice. *Am J Transplant*. 2018;18(5):1168–1176. doi:10.1111/ajt.14702
4. Burton H, Iyamu Perisanidou L, Steenkamp R, et al. Causes of renal allograft failure in the UK: trends in UK renal registry and national health service blood and transplant data from 2000 to 2013. *Nephrol Dial Transplant*. 2018;34(2):355–364. doi:10.1093/ndt/gfy168
5. Westendorp WH, Leuvenink HG, Ploeg RJ. Brain death induced renal injury. *Curr Opin Organ Transplant*. 2011;16:151–156. doi:10.1097/MOT.0b013e328344a5dc
6. Bugge JF. Brain death and its implications for management of the potential organ donor. *Acta Anaesthesiol Scand*. 2009;53:1239–1250. doi:10.1111/j.1399-6576.2009.02064.x
7. UK Renal Registry. UK Renal Registry 21st Annual Report. 2019;3349. https://www.renalreg.org/publications-reports/

8. Van Erp AC, Rebolledo RA, Hoeksma D, et al. Organ-specific responses during brain death: increased aerobic metabolism in the liver and anaerobic metabolism with decreased perfusion in the kidneys. *Sci Rep.* 2018;8(1):4405. doi:10.1038/s41598-018-22689-9

9. Akhtar MZ, Sutherland AI, Huang H, Ploeg RJ, Pugh CW. The role of hypoxia-inducible factors in organ donation and transplantation: the current perspective and future opportunities. *Am J Transplant.* 2014;14(7):1481–1487. doi:10.1111/ajt.12737

10. Akhtar MZ, Huang H, Kaisar M, et al. Using an integrated -omics approach to identify key cellular processes that are disturbed in the kidney following brain death. *Am J Transplant.* 2015. doi:10.1111/ajt.13626

11. Huang H, van Dullemen LFA, Akhtar MZ, et al. Proteo-metabolomics reveals compensation between ischemic and non-injured contralateral kidneys after reperfusion. *Sci Rep.* 2018;8(1):1–12. doi:10.1038/s41598-018-26804-8

12. Schuurs TA, Morariu AM, Ottens PJ, et al. Time-dependent changes in donor brain death related processes. *Am J Transplant.* 2006;6:2903–2911. doi:10.1111/j.1600-6143.2006.01547.x

13. Koudstaal LG, Ottens PJ, Ploeg RJ, Van GH, Brain LHGD. *Death Induces Inflammation in the Donor.* 2008;86:148–154. doi:10.1097/TP.0b013e31817ba53a

14. Bos EM, Leuvenink HGD, van Goor H, Ploeg RJ. Kidney grafts from brain dead donors: inferior quality or opportunity for improvement? *Kidney Int.* 2007;72(7):797–805. doi:10.1038/sj.ki.5002400

15. Floerchinger B, Oberhuber R, Tullius SG. Effects of brain death on organ quality and transplant outcome. *Transplant Rev.* 2012;26(2):54–59. doi:10.1016/j.trre.2011.10.001

16. Meyer-Schwesinger C. The ubiquitin–proteasome system in kidney physiology and disease. *Nat Rev Nephrol.* 2019;15(7):393–411. doi:10.1038/s41581-019-0148-1

17. Meyer-Schwesinger C, Meyer TN, Münster S, et al. A new role for the neuronal ubiquitin C-terminal hydrolase-LI (UCH-LI) in podocyte process formation and podocyte injury in human glomerulopathies. *J Pathol.* 2008;2009(217):452–464. doi:10.1002/path.2446

18. Rinschen MM, Hoppe A-K, Grahammer F, et al. N-degradomic analysis reveals a proteolytic network processing the podocyte cytoskeleton. *J Am Soc Nephrol.* 2017;28(10):2867–2878. doi:10.1681/ASN.2016101119

19. Rinschen MM, Huesgen PF, Koch RE. The podocyte protease web: uncovering the gatekeepers of glomerular disease. *Am J Physiol - Ren Physiol.* 2018;315(6):F1812–F1816. doi:10.1152/ajprenal.00380.2018

20. Fukasawa H. The role of the ubiquitin-proteasome system in kidney diseases. *Clin Exp Nephrol.* 2012;16:507–517. doi:10.1007/s10157-012-0643-1

21. Dix MM, Simon GM, Cravatt BF. Global mapping of the topography and magnitude of proteolytic events in apoptosis. *Cell.* 2008;134(4):679–691. doi:10.1016/j.cell.2008.06.038

22. Kaisar M, van Dullemen L, Charles P, et al. Subclinical changes in deceased donor kidney proteomes are associated with 12-month allograft function posttransplantation – A preliminary study. *Transplantation.* 2018;103(2):323–328. doi:10.1097/TP.0000000000002358

23. de Kok MJ, McGuinness D, Shiels PG, et al. The neglectable impact of delayed graft function on long-term graft survival in kidneys donated after circulatory death associates with superior organ resilience. *Ann Surg.* 2019:1–8. doi:10.1097/SLA.0000000000003515

24. https://www.nds.ox.ac.uk/research/quod.

25. Kaisar M, van Dullemen LFA, Thézénas M-L, et al. Plasma degradome affected by variable storage of human blood. *Clin Proteomics.* 2016;13:26. doi:10.1186/s12014-016-9126-9

26. Kaisar M, van Dullemen LFA, Thézénas ML, Charles PD, Ploeg RJ & Kessler BM. Plasma biomarker profile altered through variable blood storage. *Clin Chem.* 2016;62(9):1272–1277.

27. Fischer R, Trudgian DC, Wright C, et al. Discovery of candidate serum proteomic and metabolomic biomarkers in ankylosing spondylitis. *Mol Cell Proteomics.* 2012;11(2):M111.013904. doi:10.1074/mcp.M111.013904

28. Niessen S, Hoover H, Gale AJ. Proteomic analysis of the coagulation reaction in plasma and whole blood using PROTOMAP. *Proteomics.* 2011;11(12):2377–2388. doi:10.1002/pmic.201000674

29. Jensen MS, Mutsaers HAM, Tingskov SJ, et al. Activation of the prostaglandin E 2 EP 2 receptor attenuates renal fibrosis in unilateral ureteral obstructed mice and human kidney slices. *Acta Physiol.* 2019;227:e13291. doi:10.1111/apha.13291

30. Saleem MA, O'Hare MJ, Reiser J, et al. A conditionally immortalized human podocyte cell line demonstrating nephrin and podocin expression. *JASN.* 2002;8:630–638.

31. Farmer LK, Rollason R, Whitcomb DJ, et al. TRPC6 binds to and activates calpain, independent of its channel activity, and regulates podocyte cytoskeleton, cell adhesion, and motility. *J Am Soc Nephrol.* 2019:ASN.2018070729. doi:10.1681/ASN.2018070729

32. Dix MM, Simon GM, Cravatt BF. Global identification of caspase substrates using PROTOMAP (protein topography and migration analysis platform). *Methods Mol Biol.* 2014;1133:61–70. doi:10.1007/978-1-4939-0357-3_3

33. Feng D, DuMontier C, Pollak MR. The role of alpha-actinin-4 in human kidney disease. *Cell Biosci.* 2015;5:44. doi:10.1186/s13578-015-0036-8

34. Tian X, Kim JJ, Monkley SM, et al. Podocyte-associated talin1 is critical for glomerular filtration barrier maintenance. *J Clin Invest.* 2014;124(3):1098–1113. doi:10.1172/JCI69778

35. Moser M, Legate KR, Zent R, Fässler R. The tail of integrins, talin, and kindlins. *Science.* 2009;324:895–899. doi:10.1126/science.1163865

36. Franco SJ, Rodgers MA, Perrin BJ, et al. Calpain-mediated proteolysis of talin regulates adhesion dynamics. *Nat Cell Biol.* 2004;6(10):977–983. doi:10.1038/ncb1175

37. Goll DE, Thompson VF, Li H, Wei W, Cong J. The calpain system. *Physiol Rev.* 2003;83(3):731–801. doi:10.1152/physrev.00029.2002

38. Gabrijelcic-Geiger D, Mentele R, Meisel B, et al. Human μ-calpain: simple isolation from erythrocytes and characterization of autolysis fragments. *Biol Chem.* 2001;382(12):1733–1737. doi:10.1515/BC.2001.209

39. Abdul-Hussien H, Soekhoe RGV, Weber E, et al. Collagen degradation in the abdominal aneurysm: a conspiracy of matrix metalloproteinase and cysteine collagenases. *Am J Pathol.* 2007;170(3):809–817. doi:10.2353/ajpath.2007.060522

40. Kaminska D, Tyran B, Mazanowska O, et al. Cytokine gene expression in kidney allograft biopsies after donor brain death and ischemia-reperfusion injury using in situ reverse-transcription polymerase chain reaction analysis. *Transplant.* 2007;84(9):1118–1124. doi:10.1097/01.tp.0000287190.86654.74

41. Vaisar T, Hu JH, Airhart N, et al. Parallel murine and human plaque proteomics reveals pathways of plaque rupture. *Circ Res.* 2020;127(8):997–1022. doi:10.1161/circresaha.120.317295

42. Silva LM, Kryza T, Stoll T, et al. Integration of two in-depth quantitative proteomics approaches determines the kallikrein-related peptidase 7 (KLK7) degradome in ovarian cancer cell secretome. *Mol Cell Proteomics.* 2019;18(5):818–836. doi:10.1074/mcp.RA118.001304

43. Coppo R. Proteasome inhibitors in progressive renal diseases. *Nephrol Dial Transplant.* 2014;29(SUPPL. 1):25–30. doi:10.1093/ndt/gft271

44. Nagata M. Podocyte injury and its consequences. *Kidney Int.* 2016;89(6):1221–1230. doi:10.1016/j.kint.2016.01.012

45. Beeken M, Lindenmeyer MT, Blattner SM, et al. Alterations in the ubiquitin proteasome system in persistent but not reversible proteinuric diseases. *J Am Soc Nephrol.* 2014;25(11):2511–2525. doi:10.1681/ASN.2013050522

46. Hayek SS, Sever S, Ko Y-A, et al. Soluble urokinase receptor and chronic kidney disease. *N Engl J Med.* 2015;373(20):1916–1925. doi:10.1056/NEJMoa1506362

47. Sever S, Altintas MM, Nankoe SR, et al. Proteolytic processing of dynamin by cytoplasmic cathepsin L is a mechanism for proteinuric kidney disease. *J Clin Invest.* 2007;117(8):2095–2104. doi:10.1172/JCI32022

48. Calderwood DA, Campbell ID, Critchley DR. Talins and kindlins: partners in integrin-mediated adhesion. *Nat Rev Mol Cell Biol.* 2013;14(8):503–517. doi:10.1038/nrm3624

49. Lennon R, Randles MJ, Humphries MJ. The importance of podocyte adhesion for a healthy glomerulus. *Front Endocrinol (Lausanne).* 2014;5:1–17. doi:10.3389/fendo.2014.00160

50. Lennon R, Byron A, Humphries JD, et al. Global analysis reveals the complexity of the human glomerular extracellular matrix. *J Am Soc Nephrol.* 2014;25(5):939–951. doi:10.1681/ASN.2013030233

51. Faul C, Asanuma K, Yanagida-Asanuma E, Kim K, Mundel P. Actin up: regulation of podocyte structure and function by components of the actin cytoskeleton. *Trends Cell Biol.* 2007;17(9):428–437. doi:10.1016/j.tcb.2007.06.006

52. Henderson JM, Alexander MP, Pollak MR. Patients with ACTN4 mutations demonstrate distinctive features of glomerular injury. *J Am Soc Nephrol.* 2009;20(5):961–968. doi:10.1681/ASN.2008060613

53. Mundel P, Shankland SJ. Podocyte biology and response to injury. *J Am Soc Nephrol.* 2002;13(12):3005–3015. http://www.ncbi.nlm.nih.gov/pubmed/12444221. Accessed August 3, 2016.

54. Gu C, Yaddanapudi S, Weins A, et al. Direct dynamin-actin interactions regulate the actin cytoskeleton. *EMBO J.* 2010;29(21):3593–3606. doi:10.1038/emboj.2010.249

55. Raats CJI, van den Born J, Bakker MAH, et al. Expression of agrin, dystroglycan, and utrophin in normal renal tissue and in experimental glomerulopathies. *Am J Pathol.* 2000;156(5):1749–1765. doi:10.1016/S0002-9440(10)65046-8

56. Tadokoro S, Shattil SJ, Eto K, et al. Talin binding to integrin β tails: a final common step in integrin activation. *Science (80-).* 2003;302(5642):103–106. doi:10.1126/science.1086652

57. Calderwood DA, Ginsberg MH. Talin forges the links between integrins and actin. *Nat Cell Biol.* 2003;5(8):694–697. doi:10.1038/ncb0803-694

58. Rees DJ, Ades SE, Singer SJ, Hynes RO. Sequence and domain structure of talin. *Nature.* 1990;347(6294):685–689. doi:10.1038/347685a0

59. Moldoveanu T, Hosfield CM, Lim D, Jia Z, Davies PL. Calpain silencing by a reversible intrinsic mechanism. *Nat Struct Biol.* 2003;10(5):371–378. doi:10.1038/nsb917

60. Courdier-Fruh I, Briguet A. Utrophin is a calpain substrate in muscle cells. *Muscle Nerve.* 2006;33(6):753–759. doi:10.1002/mus.20549

61. Kim DH, Beckett JD, Nagpal V, et al. Calpain 9 as a therapeutic target in TGFβ-induced mesenchymal transition and fibrosis. *Sci Transl Med.* 2019;11(501):eaau2814. doi:10.1126/scitranslmed.aau2814

62. Tan W-J, Tan Q-Y, Wang T, Lian M, Zhang L, Cheng Z-S. Calpain 1 regulates TGF-β1-induced epithelial-mesenchymal transition in human lung epithelial cells via PI3K/Akt signaling pathway. *Am J Transl Res.* 2017;9(3):1402–1409.

63. Verheijden KAT, Sonneveld R, Bakker-van Bebber M, Wetzels JFM, van der Vlag J, Nijenhuis T. The calcium-dependent protease calpain-1 links TRPC6 activity to podocyte injury. *J Am Soc Nephrol.* 2018:ASN.2016111248. doi:10.1681/ASN.2016111248

64. Murugan R, Venkataraman R, Wahed AS, et al. Increased plasma interleukin-6 in donors is associated with lower recipient hospital-free survival after cadaveric organ transplantation. *Crit Care Med.* 2008;36(6):1810–1816. doi:10.1097/CCM.0b013e318174d89f

65. Skrabal CA, Thompson LO, Potapov EV, et al. Organ-specific regulation of pro-inflammatory molecules in heart, lung, and kidney following brain death. *J Surg Res.* 2005;123(1):118–125. doi:10.1016/j.jss.2004.07.245

66. Rafaela B, György H. Intracellular Ca^{2+} sensing : its role in calcium homeostasis and signaling. *Cell.* 2017. doi:10.1016/j.molcel.2017.05.028

67. Ono Y, Saido TC, Sorimachi H. Calpain research for drug discovery: challenges and potential. *Nat Rev Drug Discov.* 2016;15(12):854–876. doi:10.1038/nrd.2016.212

SUPPORTING INFORMATION

Additional supporting information may be found in the online version of the article at the publisher's website.